[CANCER RESEARCH 64, 6511–6523, September 15, 2004]

Nuclear Factor-κB is an Important Modulator of the Altered Gene Expression Profile and Malignant Phenotype in Squamous Cell Carcinoma

Amy Loercher,[1] Tin Lap Lee,[1] Justin L. Ricker,[1] April Howard,[1] Joel Geoghegen,[1] Zhong Chen,[1] John B. Sunwoo,[1] Raquel Sitcheran,[3] Eric Y. Chuang,[2] James B. Mitchell,[2] Albert S. Baldwin, Jr.,[3] and Carter Van Waes[1,2]

[1]Head and Neck Surgery Branch, National Institute on Deafness and Other Communication Disorders, Rockville, Maryland; [2]Radiation Oncology Sciences Program, National Cancer Institute, Bethesda, Maryland; and [3]Lineberger Cancer Center, University of North Carolina, Chapel Hill, North Carolina

ABSTRACT

We reported previously that transcription factor nuclear factor (NF)-κB is constitutively activated in human and murine squamous cell carcinomas (SCCs). The role of NF-κB in the cumulative changes in gene expression with transformation and progression of the murine SCC Pam 212 and after switching off NF-κB by a dominant negative inhibitor κB mutant (IκBαM) was explored by profiling with a 15,000-element cDNA micoarrray. Remarkably, NF-κB modulated the expression of >60% of the 308 genes differentially expressed between normal keratinocytes and metastatic SCCs. NF-κB directly or indirectly modulated expression of programs of genes functionally linked to proliferation, apoptosis, adhesion, and angiogenesis. Among these, changes in expression of cyclin D1, inhibitor of apoptosis-1, mutant Trp53, and β-catenin detected with modulation of NF-κB by microarray were confirmed by Western and Northern blot. NF-κB DNA binding motifs were detected in the promoter of ~63% of genes showing increased expression and 33% of the genes showing decreased expression. The ACTACAG motif implicated in the NF-κB-dependent down-regulation of mRNA expression of *MyoD* and *Sox9* was detected in the coding portion of about 15% of genes showing increased or decreased expression. Inactivation of NF-κB inhibited malignant phenotypic features including proliferation, cell survival, migration, angiogenesis, and tumorigenesis. These results provide evidence that NF-κB is an important modulator of gene expression programs that contribute to the malignant phenotype of SCC.

INTRODUCTION

Many cancers share a complex set of phenotypic traits, suggesting that common molecular regulatory mechanisms underlie their development (1). These traits include inhibition of programmed cell death and increased proliferation, migration, new blood vessel formation (angiogenesis), and inflammation. The resemblance of these complex phenotypic changes in cancer to those occurring transiently during the response to injury and infection suggests the hypothesis that oncogenic activation of injury response pathways and their target genes may be important in the pathogenesis of cancer. Consistent with this hypothesis, our investigations of molecular alterations in squamous cell carcinomas (SCCs) that arise from the skin and upper aerodigestive tract have revealed constitutive expression of multiple integrin cell adhesion molecules and proinflammatory cytokines that are conditionally expressed in response to injury (2, 3). A wider molecular comparison between normal, transformed, and metastatic keratinocytes by mRNA differential display and cDNA microarray revealed altered expression of an even greater diversity of genes, including genes functionally related to growth, apoptosis, adhesion, angiogenesis, and inflammation (4). We noted that a number of these cytokines, cell adhesion molecules, and other genes expressed in SCC have been associated with activation or as targets of the early injury response transcription factor, nuclear factor (NF)-κB (4–7).

NF-κB is expressed in an inactive form in most cells, composed of NF-κB p50 and Rel A p65 subunits, and bound to an inhibitory protein, IκBα (8). In response to DNA damage, cytokine, or growth factor signaling, IκBα is phosphorylated, ubiquitinated, and degraded by the proteasome, enabling nuclear localization and binding of p50/p65 to the promoter region of target genes. We established that p50/p65 is the predominant form of NF-κB constitutively activated in human head and neck and murine SCCs and that NF-κB promotes the overexpression of the proinflammatory and angiogenesis factor homologues interleukin-8 and growth regulated oncogene-1 [*Gro-1* (5, 6)]. Inhibition of NF-κB by a dominant negative IκBα phosphorylation mutant (IκBαM) or pharmacological antagonists inhibited tumor cell survival, cytokine expression, angiogenesis, and tumorigenesis by human and murine SCC (5, 7, 9, 10).

Molecular profiling of changes in gene expression with stepwise transformation and metastatic progression of SCC in the syngeneic murine Pam 212 model revealed altered expression of a diversity of genes, including a cluster of overexpressed genes in lymph node metastases (Pam LY cells) related to the NF-κB pathway (4). However, we observed that the inhibitory effects on cell survival of expression of IκBαM under a constitutive promoter made it difficult to obtain stable transfectants of Pam LY and other SCCs for the study of the role of NF-κB in gene expression and the malignant phenotype (7).

Here, we examined the overall differences in gene expression between normal, transformed, and metastatic keratinocytes using 15,000 cDNA microarrays, and we explored the role of NF-κB in the genetic and phenotypic changes acquired during tumor progression in the metastatic cells by genetically switching off NF-κB with IκBαM under control of a doxycycline [DOX (Tet)]-inducible promoter. We obtained evidence that NF-κB modulates a broad program of genes differentially expressed with tumor progression of this SCC. We further established that inhibition of NF-κB inhibited proliferation, cell survival, migration, angiogenesis, and tumorigenesis of SCC cells. These results provide evidence that NF-κB is an essential molecular switch for the gene expression program and malignant phenotype in SCC.

MATERIALS AND METHODS

Cell Lines and Culture Conditions. The murine SCC line Pam 212 was derived from spontaneously transformed BALB/c keratinocytes, and LY-2 was isolated from lymph node metastases that developed in BALB/c mice after inoculation of the parental PAM 212 SCC line (11). LY-2 has been shown to grow more aggressively and have a higher constitutive NF-κB activity than the PAM 212 line (5, 12). The SCC lines were maintained in Eagle's Minimal Essential Medium (EMEM) (Life Technologies, Inc., Grand Island, NY) with 10% fetal calf serum, 1% glutamine, and 0.5% penicillin/streptomycin at 37°C in 5% CO_2. Cell lines were determined to be *Mycoplasma*-free by nested reverse transcription-polymerase chain reaction.

Transfection of Tet-On and Tet-Inducible IκBαM Plasmids. The Tet-On expression system used was obtained from Clontech Laboratories, Inc.,

Received 3/9/04; revised 5/26/04; accepted 7/15/04.

Grant support: C. Van Waes was supported by NIDCD Intramural Project DC-00016.

The costs of publication of this article were defrayed in part by the payment of page charges. This article must therefore be hereby marked *advertisement* in accordance with 18 U.S.C. Section 1734 solely to indicate this fact.

Requests for reprints: Carter Van Waes, Head and Neck Surgery Branch, National Institute on Deafness and Other Communication Disorders, Building 10, Room 5D55, 10 Center Drive, MSC-1419, Rockville, MD 20892-0001. E-mail: vanwaesc@nidcd.nih.gov.

©2004 American Association for Cancer Research.

Downloaded from http://aacrjournals.org/cancerres/article-pdf/64/18/6511/2518426/zch01804006511.pdf by guest on 01 March 2024

(Palo Alto, CA). LY-2 cells were cotransfected with the Tet-On plasmid system containing the Tet-responsive transcriptional activator that binds the Tet-responsive element (TRE) and the gentamicin resistance gene (neo), together with the tetR plasmid that binds the TRE in the absence of DOX that reduces background levels of transcription. Cells (1.25×10^6) were plated into 100-mm dishes, incubated overnight, and transfected with 1.6 μg of the Tet-On plasmid, 14.4 μg of tetR, and 128 μL per reaction of LipofectAMINE (Life Technologies, Inc., Gaithersburg, MD) in Opti-MEM (Life Technologies, Inc., Grand Island, NY). Clones containing the Tet-On plasmid were selected by limiting dilution in 96-well plates using selection medium containing 600 μg/mL G418. Clones were expanded and screened for responsiveness to DOX using a TRE-luciferase assay. Fourteen clones with low background and high fold induction of luciferase reporter activity after the addition of 2 μg/mL DOX were selected and pooled as controls (LY-2P) and for transfection by the response plasmid containing IκBαM. The 14 LY-2 clones containing the Tet-On plasmid were transferred into 6-well plates at a concentration of 2×10^5 cells/well and incubated overnight at 37°C. The cells were transfected with 1 μg of TRE-IκBαM plasmid (pTRE-Igs32s36 from Clontech Laboratories, Inc.), 4 μL of LipofectAMINE, and 6 μL of PLUS reagent (Life Technologies, Inc., Gaithersburg, MD) per reaction in Opti-MEM. Reactions were incubated for 5 hours at 37°C in 5% CO_2. The medium was changed to complete EMEM (Life Technologies, Inc.), and cells were allowed to recover overnight. To select subclones containing both the Tet-On and TRE-IκBαM plasmids, transfectants were diluted 1:40 for subcloning using one 200-mm dish for each clone. After 7 days in EMEM containing 600 μg/mL G418, colonies were selected using cloning cylinders (Genechoice, Frederick, MD), and four subclones from each dish, labeled A to D, were transferred to a 24-well plate and expanded for screening for Tet-inducible expression of IκBαM by Western blot, as described previously (5).

Nuclear Factor-κB Luciferase Assay. Four clones selected for expression of IκBαM by Western blot and the LY-2P parent cells were transferred to triplicate wells at a concentration of 2×10^5 cells/well in 6-well tissue culture plates. Cells were incubated overnight at 37°C and then transfected with 0.95 μg of NF-κB luciferase plasmid, 4 μL of LipofectAMINE, and 6 μL of PLUS reagent in 1 mL of Opti-MEM per well for 5 hours at 37°C. The transfection medium was replaced with complete EMEM, and cells were incubated until they reached 80% confluence. NF-κB-luciferase assays were performed as described previously (10).

Electromobility Shift Assay. Double-stranded DNA probes for NF-κB (5′-AGTTGAGGGGACTTTC-CCAGGC-3′) and Oct-1 (5′-TGTCGAATG-CAAATCACTAGAA-3′) were commercially obtained (Promega, Madison, WI). Probes were labeled with [γ-^{32}P]ATP (6000 Ci/mmol; Amersham, Arlington Heights, IL). Nuclear extracts were prepared from DOX-treated and untreated LY-2 IκBαM clones, and DNA binding assays were performed with 5 μg of nuclear extracts using standard methods described previously (5).

Microarray Analysis. Total RNA was isolated from primary BALB/c keratinocytes, Pam 212, and LY-2 cells and the LY-2P and the four inducible LY-2 IκBαM clones (23D, 24C, 25D, and 26C) with and without DOX treatment. RNA was collected 72 hours after DOX treatment in three independent experiments. The 15,000-element murine microarray developed by the Radiation Oncology Sciences Program, National Cancer Institute, using a cDNA library from the National Institute of Aging (Mm-ROSP-NIA15K), was used.[4] Sequential arrays were obtained from two different printings. Experiments were performed in triplicate. The protocols used for RNA isolation, hybridization, and microarray analysis were those available from the National Human Genomics Research Institute.[5] Arrays were read on a Genepix 4000B Scanner, and data were collected using Genepix Pro 4.0 software (Axon Instruments, Foster City, CA).

Statistical and Bioinformatic Analyses. Array elements exhibiting mean signal differences of ≥2-fold (99% confidence interval) for triplicate comparisons among cDNAs from normal keratinocytes, transformed Pam 212, and/or metastatic Pam LY-2 cells were scored as being associated with tumor progression. Array elements exhibiting reversion of mean differences of ≥2-fold (99% confidence interval) for comparisons among cDNAs from metastatic Pam LY-2P and four LY-2 IκBαM clones ± DOX were scored as putative NF-κB-modulated genes. Analysis of the collected data was performed using the Cluster and Treeview software developed by Michael Eisen (Stanford University), as described previously (4). Genes were assigned to functional families based on information from LocusLink and PubMed. Sequence data generated through the use of the Celera Discovery System and verified in public databases were used for detection of NF-κB–related motifs. The sequences from 2 kb 5′ and the full-length of each gene found to be differentially expressed by microarray were examined for NF-κB binding motifs (12) by Genomatix software and for ACTACAG motifs involved in NF-κB–mediated down-regulation of *MyoD* and *Sox9* mRNA (13) by BLAST search available from the National Center for Bioinformatics, National Institutes of Health.

Northern Blot. RNA isolated for microarray analysis was subjected to electrophoresis and Northern blot as described previously (4). Blots were probed with full-length ^{32}P-labeled DNA probes for the *cyclin D1*, *Trp53*, inhibitor of apoptosis-1 (*IAP-1*), *β-catenin*, and *β-actin* genes and washed under high stringency conditions.

Whole Cell Lysates and Western Blot. Whole cell lysates were collected from DOX-treated and untreated IκBαM clones in 6-well plates after washing twice with PBS and addition of 300 μL of lysis buffer [100 mmol/L potassium phosphate, 0.2% Triton X-100, and 0.05% dithiothreitol (Tropix; PE Biosystems, Bedford, MA)] to each well. Plates were held at 4°C for 1 hour and then subjected to three freeze-thaw cycles. Lysates were transferred to 2-mL microtubes and centrifuged for 5 minutes at 13,000 rpm. Lysates were diluted 1:10 in distilled H_2O and analyzed for protein content by the BCA protein assay kit (Pierce, Rockford, IL). Samples were stored at −80°C until use. Twenty micrograms of protein were loaded onto precast 12% Tris-glycine gels (Novex, San Diego, CA). Gels were run for 2 hours at 100 V, and then proteins were transferred to nitrocellulose membranes for 90 minutes at 20 V. Membranes were blocked in 5% milk in Tris-buffered saline at 4°C overnight. For selection of clones expressing IκBαM after DOX treatment, blots were incubated for 2 hours at 4°C in a 1:200 dilution of anti-IκBα (rabbit polyclonal antibody; Santa Cruz Biotechnology, Santa Cruz, CA). Antibodies recognizing cyclin D1, Trp53, IAP-1, β-catenin, and β-tubulin proteins were obtained from Santa Cruz Biotechnology. Membranes were washed and incubated for 1 hour at room temperature in a 1:3,000 dilution of goat antirabbit antibody labeled with horseradish peroxidase (Santa Cruz Biotechnology). Membranes were washed, enhanced with SuperSignal chemiluminescence reagent (Pierce), placed in heat-sealable pouches (Kapak, Minneapolis, MN), and exposed to film.

MTT Cell Proliferation Assay. Proliferation of LY-P and the IκBαM clones was measured using a 3-(4,5-dimethylthiazol-2-yl)-2,5-diphenyltetrazolium bromide (MTT) cell proliferation kit (Roche Molecular Biochemicals, Mannheim, Germany). Cells were transferred in triplicate to a 96-well, flat-bottomed plate at a concentration of 5×10^3 cells/well in 100 μL of complete EMEM with or without DOX. Cells were incubated at 37°C in 5% CO_2 for 1, 3, or 5 days, and growth rates were analyzed after the addition of MTT reagent to the cultured cells and lysis according to the manufacturer's instructions. Absorbance was determined using multichannel spectrophotometry at a wavelength of 570 nm.

Cell Cycle Analysis. LY-2P, 23D, and 24C cells were transferred to 6-well plates at a concentration of 5×10^5 cells/well and treated with 2 μg/mL DOX or left untreated. After 96 hours, floating and adherent cells were collected and counted. One million cells were washed twice in buffer solution from the CycleTest Plus DNA Reagent Kit (Becton Dickinson, San Jose, CA) and then resuspended in 250 μL of trypsin buffer. Cells were incubated for 10 minutes at room temperature. Two hundred microliters of trypsin inhibitor/RNase buffer were added to each tube, and cells were incubated for 10 minutes at room temperature. Two hundred microliters of cold propidium iodide staining solution were added. Cells were incubated for 10 minutes in the dark on ice, and within 3 hours of staining, quantification of DNA was determined on a FACScan flow cytometer using CellQuest software (Becton Dickinson).

Invasion Assays. Invasion assays were performed using a synthetic basement membrane cell invasion assay kit (Chemicon, Temecula, CA). Cells were plated at a concentration of 0.5×10^6 cells/mL in serum-free EMEM into the inserts of a cell invasion assay plate. Plates were incubated at 37°C in 5% CO_2 for 72 hours. Cells on the interior of the inserts were removed by swabbing, and the exterior of the inserts was stained for evidence of cell migration through the synthetic basement membrane. Stained cells were solubilized in 10% acetic acid, and the intensity of staining was quantified by transfer of

[4] http://nciarray.nci.nih.gov.
[5] http://research.nhgri.nih.gov/microarray/Protocols.pdf.

Downloaded from http://aacrjournals.org/cancerres/article-pdf/64/18/6511/2518426/zch01804006511.pdf by guest on 01 March 2024

100-μL aliquots to a 96-well plate for spectrophotometry at a wavelength of 570 nm.

Determination of Tumor Growth and Microvessel Density in Severe Combined Immunodeficient Mice. LY-2P cells (5×10^6) as a control and LY-2 24C cells were inoculated in 200 μL of serum-free EMEM subcutaneously into the flanks of congenic male BALB/c severe combined immunodeficient (SCID) mice (5 mice per group). Animals received water treated with 2 μg/mL DOX beginning at week 7. Tumor measurements were recorded once a week for the duration of tumor growth to 10 weeks. After euthanasia, tumors were harvested, prepared for frozen section, and stained with hematoxylin and eosin (H&E) or antibody specific for CD31 as described previously (9).

RESULTS

Inhibition of Nuclear Factor-κB in Squamous Cell Carcinoma by Tet-Inducible IκBαM. A stepwise model of cancer development and progression was established previously from syngeneic BALB/c mice consisting of normal keratinocytes (KER), a transformed SCC cell line (Pam 212), and SCC lymph node metastases, designated Pam LY (4, 11). Pam 212 cells produce slowly growing SCC that rarely metastasizes, and Pam LY cells isolated from rare lymph node metastases of Pam 212 are variants that form cancers that grow and metastasize rapidly. Molecular comparisons between these normal, transformed, and metastatic keratinocytes by mRNA differential display and a first-generation 4,000-element cDNA microarray provided evidence for altered expression of multiple genes related to growth, apoptosis, angiogenesis, inflammation, and the NF-κB pathway (4).

To directly explore the role of NF-κB in the accumulated changes in gene expression acquired with tumor progression of Pam LY, we sequentially transfected plasmids containing a TRE and the IκB signal mutant IκBαM under the control of a DOX-inducible promoter into the Pam LY-2 line, a representative metastatic line that exhibits constitutive activation of NF-κB (5). Multiple LY-2 cell clones that showed low background and high inducibility by the Tet derivative DOX in a Tet reporter assay after first-stage transfection were pooled for transfection by the Tet-IκBαM construct and for use as controls. Expression of IκBαM by LY-2 clones was detected by Western blot as described previously (5), and four clones that exhibited low basal and strong DOX-induced expression of IκBαM were selected to examine effects on NF-κB activation. The effect of DOX-induced IκBαM expression on constitutive NF-κB-luciferase reporter gene activity in the four LY-2 subclones and LY-2P control lacking Tet-IκBαM is shown in Fig. 1*A*. IκBαM inhibited NF-κB functional promoter activity as determined using NF-κB-luciferase reporter assay (Fig. 1*A*). Progressive inhibition of constitutive NF-κB reporter activity to <95% of baseline was observed by day 4 after addition of DOX to LY-2 IκBαM clones. NF-κB reporter activity in control LY-2P cells lacking Tet-IκBαM was not suppressed below control levels (Fig. 1*A*). IκBαM also suppressed NF-κB DNA binding activity in nuclear extracts of LY-2 clones in electromobility shift assay (Fig. 1*B*). The specificity and composition of constitutive NF-κBp50/Rel Ap65 DNA binding activity in LY-2 cells were reported previously (5).

Molecular Profile of Genes Related to Tumor Progression and Nuclear Factor-κB in Squamous Cell Carcinoma. To directly explore the alterations and role of NF-κB in gene expression with tumor progression, we used the National Cancer Institute 15,000-element cDNA microarray expressing known genes to examine the diversity of genes differentially expressed among keratinocytes, transformed Pam 212, and metastatic Pam LY-2 (Met) SCC cells, and we determined the effect of conditionally inhibiting NF-κB in Pam LY-2 cells by expressing IκBαM. Complementary DNA was prepared from mRNA from three independent preparations of keratinocytes, Pam 212, and Pam LY-2 cells and from four Pam LY-2 clones expressing IκBαM after culture with DOX for 72 hours. Messenger RNA was isolated at 72 hours based on the ≥75% inhibition of NF-κB reporter activity detected in Fig. 1 and to minimize cell death or RNA degradation, which was observed beyond 96 hours (Figs. 3 and 5; data not shown). Fig. 2 shows the cluster analysis for 308 genes (*horizontal rows*) that exhibited ≥2-fold difference in expression among keratinocytes (Ker), transformed Pam 212 (Trans), or metastatic

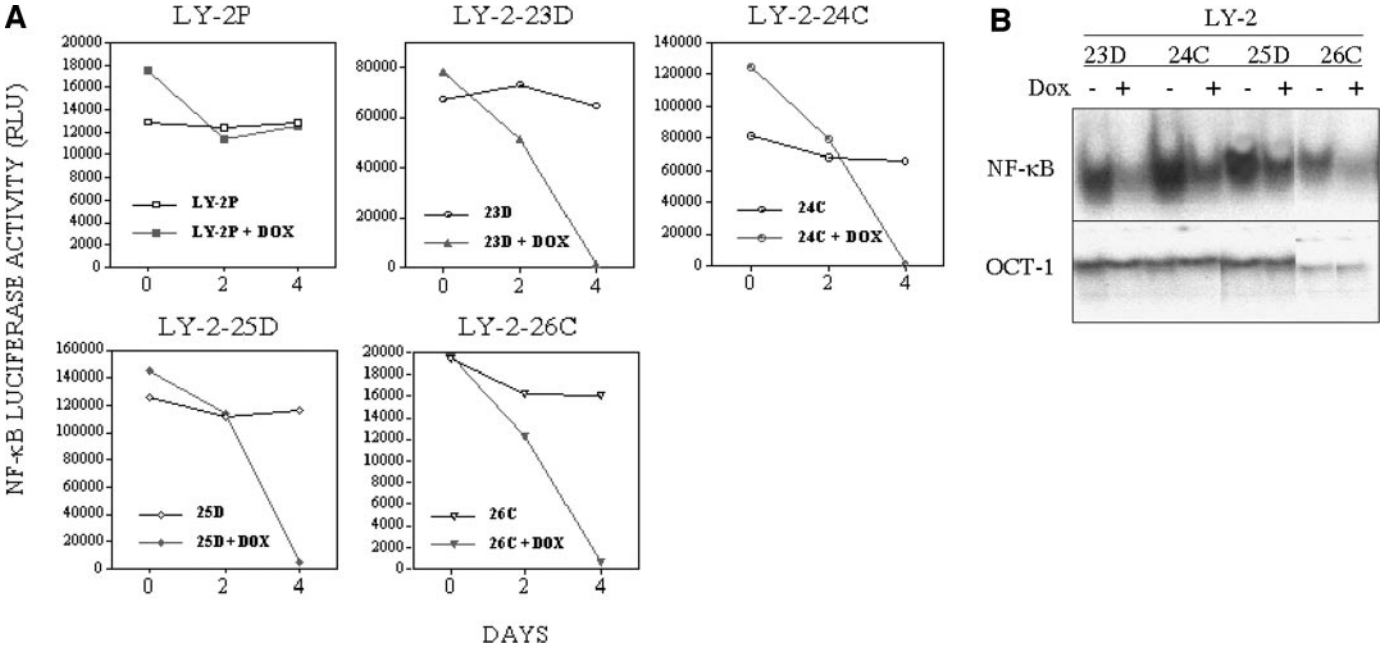

Fig. 1. Inhibition of NF-κB in LY-2 SCC clones by Tet-inducible IκBαM. *A*, NF-κB-luciferase reporter assay. LY-2P pooled control clones and LY-2 Tet-IκBαM clones 23D, 24C, 25D, and 26C were transfected with a NF-κB-luciferase reporter and incubated ± DOX as described in Materials and Methods. NF-κB-luciferase reporter activity measured on days 0, 2, and 4 is shown. *B*, NF-κB DNA binding assay. LY-2 Tet-IκBαM clones 23D, 24C, 25D, and 26C were incubated ± DOX for 72 hours, and cell extracts were subjected to electromobility shift assay with consensus NF-κB or control Oct-1–specific oligonucleotides as described. The specificity and composition of constitutive NF-κBp50/Rel Ap65 DNA binding activity in LY-2 cells were reported previously (5).

Downloaded from http://aacrjournals.org/cancerres/article-pdf/64/18/6511/2518426/zch01804006511.pdf by guest on 01 March 2024

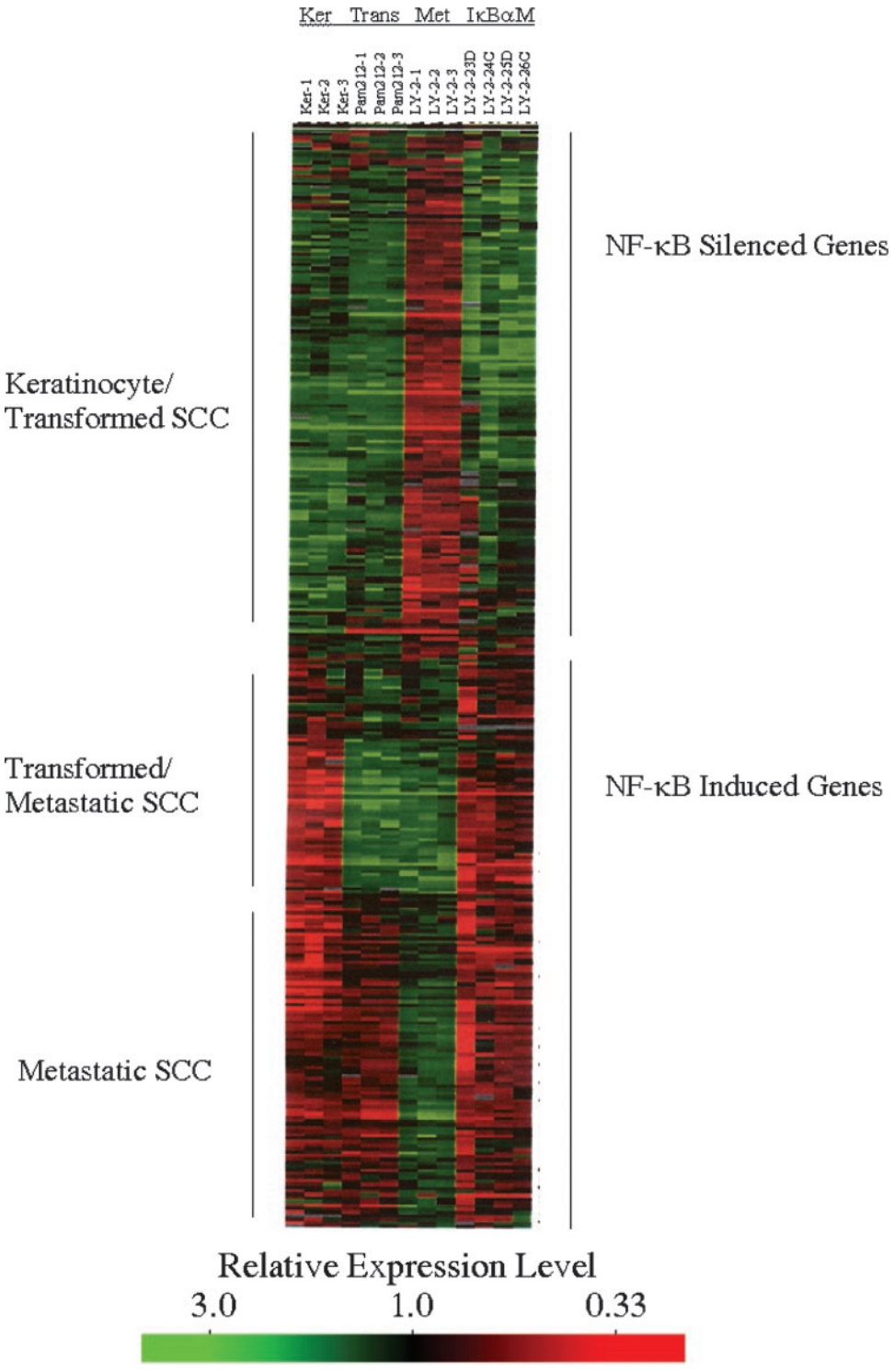

Fig. 2. Cluster analysis of genes related to tumor progression and NF-κB in SCC. Complementary DNA was prepared from mRNA from three independent preparations of keratinocytes, Pam 212, and Pam LY-2 cells and four Pam LY-2 clones expressing IκBαM after culture with DOX for 72 hours. A total of 308 of 15,000 cDNA microarray elements exhibited mean signal differences of ≥2-fold (99% confidence interval) for triplicate comparisons between cDNAs from normal keratinocytes (Ker), transformed Pam 212 (Trans), and/or metastatic Pam LY-2 (Met) cells. Three dominant patterns were detected that clustered according to the stepwise differences in phenotype among KER, Pam 212, and Pam LY-2 cells. Cluster 1 genes showed similar profiles in keratinocytes and transformed Pam 212 cells (*green*) but reduced expression in metastatic LY-2 cells (*red*). Cluster 2 genes showed lower expression in normal cells (*red*) but increased expression in transformed and metastatic cells (*green*). Cluster 3 genes showed low intensity in keratinocytes and transformed cells (*red*) and increased signal intensity primarily in LY-2 metastatic cells (*green*).

Pam LY-2 (Met) cells and Pam LY-2 cells expressing IκBαM after DOX (*vertical columns*). Overall, the differential pattern of expression detected for 308 of 15,000 of the gene elements on the array represents about 2% of the genes compared. Three dominant patterns were detected that clustered according to the stepwise differences in phenotype among KER, Pam 212, and Pam LY-2 cells. Cluster 1 genes showed similar expression in normal and transformed Pam 212 cells but reduced expression in metastatic LY-2 cells. Cluster 2 genes showed lower expression in normal cells but increased expression in transformed and metastatic cells. Cluster 3 genes showed increased expression primarily in LY-2 metastatic cells. Overall, 141 genes in the upper cluster showed a decrease, and 167 genes in clusters 2 and 3 were increased in association with transformation, tumor progression, and activation of NF-κB.

Tables 1 and 2 show a selected list from the 308 genes detected by microarray and cluster analysis that exhibited ≥2-fold difference in hybridization with malignant progression and/or inhibition of NF-κB (the full list is available online).[6] Table 1 includes the genes that show

[6] http://www.nidcd.nih.gov/research/scientists/vanwaesc.asp.

Downloaded from http://aacrjournals.org/cancerres/article-pdf/64/18/6511/2518426/zch01804006511.pdf by guest on 01 March 2024

Table 1 *Selected list of genes increased with tumor progression*

Function Gene	Symbol	Clone ID	NF-κB association	Fold change LY-2/Ker	Fold change LY-2/IκB-αM
Cell cycle/growth					
*Cyclin D1**	*Ccnd1*	H3084D05	Target gene	3.351	−2.266
*Cyclin D2**	*Ccnd2*	H3152D01	Target gene	2.957	−2.05
*Growth arrest specific 5**	*Gas5*	H3113A12		6.304	−7.813
*Milk fat globule-EGF factor 8**	*Mfge8*	H3126F11	Target gene	2.594	−3.525
Protein phosphatase 3†*	*Ppp3cb*	H3065C08	Inhibitor of NF-κB	3.117	−2.231
*Proliferating cell nuclear antigen**	*Pcna*	H3021F12	Target gene	5.775	−2.811
Apoptosis					
*Baculoviral IAP repeat**	*Birc2*	H3074A02	Target gene	9.154	−6.013
Bcl-2 related ovarian killer†*	*Bok1*	H3081D02		1.994	−3.461
*Immediate early response 3**	*Ier3*	H3057B07	Target gene	2.865	−3.851
Transformation related protein†*	*Trp53*	H3142D07	Target gene	2.9	−4.142
Uchrp†	*Uchrp*	IMAGE:605056		2.188	−4.353
Inflammation/angiogenesis					
*Colony stimulating factor 1**	*Csf1*	H3057D05	Target gene	14.639	−5.574
Complement component 3†*	*C3*	H3054A08	Target gene	5.145	−8.303
*FGF receptor**	*Fgfr4*	IMAGE:406823	Target gene	1.982	−1.991
*Gro 1 oncogene**	*Gro1*	H3051F10	Target gene	12.394	−4.094
*Histocompatibility 2-L**	*H2-L*	H3096A12	Target gene	2.342	−3.431
*Histocompatibility 2-D**	*H2-D*	H3141B11	Target gene	2.968	−3.927
*Interferon receptor**	*Ifnar*	H3118F09	Inhibitor of NF-κB	4.5	−3.054
*Lymphocyte antigen complex**	*Ly6e*	H3027D05	Inducer of NF-κB	4.029	−2.613
Metastasis					
Integrin α 3†*	*Itga3*	H3137A03	Inducer of NF-κB	15.597	−3.917
Laminin α 5†*	*Lama5*	H3002G01	Target gene	2.272	−2.967
Laminin receptor 1	*Lamr1*	H3075G08		2.169	−1.619
Plasminogen activator, tissue	*Plat*	H3080H11	Target gene	2.667	−2.487
Procollagen type 5 α 2	*Col5a2*	H3156E09	Target gene	5.103	−2.094
*Syndecan 1**	*Sdc1*	H3013F05	Target gene	2.948	−2.034
Metabolism					
ATPase H^+ transport†*	*Atp6b*	H3120H04	Inhibitor of NF-κB	2.247	−2.858
*Branched chain ketoacid dehyd**	*Bckdk*	H3136B09		2.455	−3.042
Choline kinase†*	*Chk*	H3088E07	Inducer of NF-κB	6.662	−3.252
*Cytochrome p450**	*Cyp1b1*	J0216F07	Target gene	22.289	−4.286
*Glutathione-S-transferase**	*Gstm1*	H3133A06	Target gene	3.037	−3.061
*Low density lipoprotein receptor**	*Ldlr*	H3014C04	Target gene	2.689	−3.226
Mannose-6-phosphate receptor†	*M6pr*	H3092C05	Inhibitor of NF-κB	6.303	−3.612
*Potassium intermediate**	*Kcnn4*	H3054H04		2.778	−2.197
Solute carrier family 12†*	*Slc12a2*	H3077B02		2.551	−2.145
Stress response					
*Heat shock protein, 70 kDa**	*Hspa5*	H3032A08	Activates NF-κB	14.303	−6.369
*Heat shock protein 84 kDa**	*Hsp84*	H3042G07	Activates NF-κB	3.437	−7.198
*Heat shock protein 86 kDa**	*Hsp86*	H3023G01	Activates NF-κB	2.61	−2.34
*Heat shock protein cognate 70**	*Hsc70*	H3133H01	Binds NF-κB	3.42	−10.229
*Superoxide dismutase**	*Sod1*	H3130B11	Target gene	4.784	−2.145
Signal transduction					
AXL receptortyrosine kinase†*	*Axl*	H3152F05	Inhibitor of NF-κB	2.459	0.938
CD97 (EGF-TM7)†*	*Cd97*	H3032G06		2.283	−1.352
*Interleukin-1 receptor associated**	*Il1rak*	H3042E08	Activates NF-κB	1.999	−1.296
Frizzled 7 homolog	*Fzd7*	H3031A03		2.717	−0.843
*Growth arrest & DNA damage specific**	*Gadd45g*	H3054C02	Activates NF-κB	3.144	−1.407
*Growth factor receptor bound**	*Grb2*	H3153D02	Activates NF-κB	2.483	−2.341
*N-myc downstream regulated**	*Ndr2*	G0110H06	Inhibits p50	2.248	−2.039
*PI3 kinase regulatory**	*Pik3r1*	H3067B08	Activates NF-κB	4.206	−3.539
Protein tyrosine phosphatase†*	*Ptpn13*	H3118G02	Inhibitor of NF-κB	2.844	−9.071
Ras p21 protein activator 3†*	*Rasa3*	H3054E01	Activates NF-κB	3.223	−2.71
*Ras-related C3**	*Rac1*	IMAGE:477981		2.042	−3.875
*Transferrin receptor**	*Trfr*	H3059G03		2.216	−1.145
Nuclear proteins/transcription factors					
Activating transcription factor†	*Atf2*	J0221F08		1.606	−2.696
Breast cancer, early onset†	*Brca2*	H3069F08		2.216	−0.604
*Butyrate response factor**	*Brf2*	H3015E08		2.072	−2.008
*High mobility group AT**	*Hmga1*	H3029B11	Target gene	2.816	−2.591
*Jerky**	*Jrk*	H3119F06		2.849	−3.329
*Myelocytomatosis oncogene**	*Myc*	H3089H11	Target gene	2.224	−2.42
*Nuclear factor κB p105**	*Nfkb1*	H3072E09		2.919	−1.443
Sex comb on midleg-like 1†	*Scml1*	H3113B01		2.355	−1.154
Yes-associated protein 65 kDa	*Yap*	H3089H07		2.072	−1.746
RNA processing					
*DEAD box protein 3**	*Ddx3*	H3018F11		2.976	−2.055
DJ-1 protein†	*DJ-1*	H3150D06		3.155	−4.611
FGF inducible 14	*Fin14*	H3018G01		2.358	−3.355
Nuclear ribonuclease	*Hnrpa1*	H3111H11		4.926	−2.785
*RNA polymerase 1-1**	*Rpo1-1*	H3049D09		2.703	−2.328
Protein synthesis/modification					
ERO1 like†*	*Ero1l*	H3126B01		2.529	−2.456
Ribosomal protein L27a	*Rpl27a*	H3009B05		2.183	1.369
Ribosomal protein L8	*Rpl8*	H3141F09		2.778	1.005
*Ribosomal protein S18**	*Rps18*	H3006C11		2.487	−2.424
Ubiquitin activating enzyme E1	*Ube1x*	H3022E03	Phosphorylates IκB	5.313	−3.139

Downloaded from http://aacrjournals.org/cancerres/article-pdf/64/18/6511/2518426/zch01804006511.pdf by guest on 01 March 2024

Table 1 *Continued*

Function Gene	Symbol	Clone ID	NF-κB association	Fold change LY-2/Ker	Fold change LY-2/IκB-αM
Ubiquitin B	Ubb	H3138A08	Labels IκB	8.144	−1.171
Ubiquitin conjugating enzyme E2	Ube2h	H3057B09	Ubiquitinates IκB	3.333	−1.199
Ubiquitin conjugating enzyme E3†	Ube3a	H3102B01	Ubiquitinates IκB	4.878	−5.096
Ubiquitin specific protease 9†	Usp9x	H3139F12		3.769	−3.175
Structural proteins					
Alpha tropomyosin*	Tpm1	H3120G06	Binds p65	2.421	−4.36
Cadherin*	Cdh3	H3018F05	Inflammatory	2.328	−2.706
Capping protein alpha 2	Cappa2	H3085F12		14.293	−7.458
Dystroglycan 1*	Dag1	H3008B05	Activates NF-κB	2.593	−4.738
Epithelial protein lost*†	Eplin	H3153C05	Activates NF-κB	2.066	−2.971
Fascin homolog 1*	Fscn1	H3006D08		2.315	−2.581
Four and a half LIM domains*	Fhl2	H3033C07		2.169	−1.189
Keratin complex 1 acidic*	Krt1-18	H3021B02	Target gene	3.105	−5.517
Keratin complex 2 basic*	Krt2-8	H3031C01		2.094	−5.568
PDZ and LIM domain 1*	Pdlim1	J0824B03		5.7	−3.775
Protocadherin 7*†	Pcdh7	H3067F12	Inflammatory	6.556	−1.026
Thymopoietin*	Tmpo	H3096B08		9.939	−8.153
Other					
Globin inducing factor†	Gbif	H3053F12		2.003	1.002
Metallothionein 2	Mt2	H3013D11	Inhibits IκB degradation	2.145	−3.029
Next to the Brca1*†	Nbr1	H3061D04		2.367	−1.888
RAN binding protein*	Ranbp9	H3013A10	Accumulates IκBα	2.87	−3.189
Repeat family 3 gene*	Llrep3	H3107F07		3.556	−7.704
Ring finger protein 19*	Rnf19	H3153A08	Activates NF-κB	2.148	−4.402
Sema domain, immunoglobin*†	Sema3f	H3134D09		2.191	−1.667
Suppressor of Lec15†	Supl15h	H3090D12		2.001	−1.383
TGF beta inducible transcript*	Tgfb1i1	H3122H01		3.068	−2.974

NOTE. Total number of genes regulated by NF-κB = 105/167. Total number of genes previously associated with NF-κB = 67/167.
* Genes containing κB site in promoter region.
† Genes containing ACTACAG motif in coding sequence.

increased hybridization, and Table 2 includes the genes that show decreased hybridization by cDNA of Pam 212 and/or LY-2 cells. The genes were classified according to putative function and published associations with NF-κB as determined by search of National Center for Biotechnology Information PubMed and LocusLink. The ratio of LY-2 to keratinocyte hybridization, representing the overall change with malignant progression, and the ratio of LY-2 to LY-2 IκBαM, representing the effects of expression of IκBαM, are shown. The genes that are modulated by ≥2-fold by IκBαM are shown in bold.

Remarkably, Fig. 2 and Tables 1 and 2 reveal that expression of IκBαM in Pam LY-2 results in restoration of the pattern of expression observed for keratinocytes for many of the genes up- and down-regulated between keratinocytes and Pam LY-2 metastatic cells. Of the genes up-regulated in LY-2 cells, hybrization of 115 of 167 (69%) decreased by ≥2-fold toward normal levels after expression of IκBαM. Fully 88 of 141 (62%) genes down-regulated in LY-2 cells were restored by ≥2-fold back toward the level observed in keratinocytes after expression of IκBαM. The effect of IκBαM to up-modulate as well as down-modulate mRNAs provides evidence that the wide effect on gene expression is not merely due to degradation of mRNA during the process of cell death, and we verified the viability of cells and integrity of mRNA after 72 hours of exposure to DOX (data not shown).

Corroboration between the Gene Profile Expressed in LY-2 Cells and Previously Identified Squamous Cell Carcinoma-Related Genes. As an initial assessment of the consistency and validity of the differential gene expression profile obtained for LY-2-expressing cells using the 15,000-element cDNA microarray, we identified genes that were previously found to be differentially expressed in multiple LY metastasis cell lines by a first-generation 4,000-element murine cDNA microarray and confirmed by reverse transcription-polymerase chain reaction and/or Northern blot analysis (4). Several genes in Table 1 that were classified as increased in LY-2 cells by ≥2-fold were included and detected in both array studies. These include the increase in expression of proliferation and antiapoptosis-related genes *cyclin D1* (*Ccnd1*), *proliferating cell nuclear antigen* (*Pcna*), *inhibitor of apoptosis-1* (*IAP-1/Birc-2*), and *growth arrest-specific-5* (*Gas5*); inflammatory factors and receptors *growth-regulated oncogene 1* (*Gro-1/KC*), *colony-stimulating factor-1* (*csf1*), *complement 3* (*C3*), and *lymphocyte antigen 6e* (*Ly6e*); metabolism and drug resistance genes *cytochrome P450* (*Cyp1b1*) and *glutathione S-transferase* (*Gstm1*); signal molecules *protein tyrosine phosphatase* (*Ptpn13*) and *Yes-associated protein 65 kDa* (*Yap65*); and chromatin-associated *high mobility group protein* [*Hmga1* (4)]. Of these, differential expression in LY-2 cells and two other LY lines was also confirmed previously by Northern blot for *Gas5*, *Gro-1/KC*, *Ly6*, *Gstm1*, and *Yap65* (4, 14). Several genes in Table 2 that were classified as decreased in LY-2 cells by ≥2-fold were also detected using both arrays. These include *cyclin-dependent kinases 1 and 4 (Cdkn1* and *Cdk4*), *calmodulin* (*Calm*), *cadherin 1* (*Cdh 1*), *prothymosin b4* (*Ptmb4*), *mucin* (*muc18*), *procollagens type I and IVα* (*Col1a2* and *Col4a2*); *ATPase* (*Atp11a*), and *creatine kinase* (*Ckmt1*). Decreased expression of *Ptmb4* was confirmed previously by Northern blot (4). Two elements showed discordant expression between the two studies, *tropomyosin α* (*Tpm1*) and *A disintegrin/MMP* (*Adamts-1*). Overall, a consistent pattern of expression was observed for the majority of elements found to be differentially expressed by cDNA hybridization in these independent studies and for six of eight genes confirmed by Northern blot (4).

Effect of IκBαM on Expression of Cyclin D1, Trp53, Inhibitor of Apoptosis-1, and β-Catenin. Changes in expression of several of the genes classified by microarray as differentially expressed in LY2 cells and modulated in LY2 IκBαM-expressing cells have been detected with oncogenesis and metastatic progression of SCC. *Cyclin D1*, *IAP-1*, and mutant *Trp53* have been reported to be overexpressed in advanced SCC, and β-catenin expression has been reported to be decreased in advanced SCC, consistent with the expression profile for these genes in LY-2 cells (Tables 1 and 2). *Cyclin D1*, *Trp53*, and *IAP-1* may be up-regulated with NF-κB in other cancer lines, and *β-catenin* may be down-regulated with NF-κB in other cancer lines

Downloaded from http://aacrjournals.org/cancerres/article-pdf/64/18/6511/2518426/zch01804006511.pdf by guest on 01 March 2024

Table 2 *Selected list of genes decreased with tumor progression*

Function Gene	Symbol	Clone ID	NF-κB association	Fold change LY2/Ker	Fold change LY2/IκB-αM
Cell cycle/growth					
*C-src tyrosine kinase**	*Csk*	L0237H04		−2.693	2.358
Calmodulin	*Calm*	H3006H05	Activates NF-κB via IKK	−2.554	2.42
Cell division cycle homolog 25a	*Cdc25a*	H3050E04		−2.341	2.269
Cell division cycle homolog 45	*Cdc45l*	H3003E07		−2.032	2.029
Cyclin C	*Ccnc*	C0117F09		−2.739	2.418
*Cyclin E2**	*Ccne2*	C0186A01		−2.309	2.155
Cyclin dependent kinase 4	*Cdk4*	H3147D06	Target gene of NF-κB	−2.734	2.05
*Cyclin dependent kinase inhibitor**	*Cdkn1c*	H3097D03		−5.208	2.913
*Platelet derived growth factor**	*Pdgfa*	H3146C02		−2.15	2.906
Apoptosis					
*ATP binding cassette**	*Abcd3*	H3143E03	NF-κB site in promoter	−2.89	2.535
Bcl2/adenovirus E1B	*Bnip3*	H3103B07	Transient inhibitor of NF-κB	−2.364	2.436
Fas associating w/ death domain	*Fadd*	H3095D08	Inducer of NF-κB	−3.597	2.975
Inflammation/angiogenesis					
Coagulation factor III†*	*F3*	H3014G02	Activates NF-κB via IKK	−4.672	3.858
Interleukin 17 receptor	*Il17r*	H3008A03	Activates NF-κB via MAPK	−3.021	3.048
Interleukin 2 receptor	*Il2ra*	J0052C08		−2.262	2.207
Lymphocyte antigen 6 complex	*Ly6*	H3115A08	Inducer of NF-κB	−5.617	3.311
Prothymosin β	*Ptmb4*	H3143A02		−21.739	8.858
Metastasis					
A disintegrin/MMP	*Adamts1*	H3034B07		−2.695	2.736
*Cadherin 1**	*Cdh1*	H3076B06	Associated with inflammation	−2.597	2.313
Kangai 1†	*Kai1*	H3154D02	Target gene of NF-κB	−2.816	2.139
Lipocalin 2	*Lcn2*	H3083G02	Associated with inflammation	−2.506	11.235
Procollagen type 1 α	*Col1a2*	H3125D01		−4.901	2.886
Procollagen type II α	*Col2a1*	H3026G09		−6.896	2.139
Procollagen type III α	*Col3a1*	H3005D11	Inducer of NF-κB	−3.205	4.268
Secreted acidic C-rich	*Sparc*	H3026D08		−8.928	2.872
Tissue inhibitor of MMPs	*Timp3*	H3031E01		−3.3	3.289
Metabolism					
ATPase, type 11A†	*Atp11a*	H3097B05		−2.888	2.734
ATP synthase H^+ transport	*Atp5j2*	H3118C01	Inhibitor of NF-κB upregulates IκBα normal half-life	−2.191	2.111
*Glutathione peroxidase**	*Gpx3*	J0088G08		−2.604	4.065
Lipopolysaccharide binding†*	*Lbp*	H3086G08	Activates NF-κB via MAPK	−2.977	2.103
Phosphoprotein enriched†	*Pea15*	H3014G07	Inducer of NF-κB	−2.424	1.159
Pyruvate dehydrogenase†*	*Pdha1*	H3068G07	NF-κB site in promoter	−3.021	1.643
Sterol carrier protein 2†*	*Scp2*	H3122F12		−2.412	1.488
Stress response					
Crystallin α 2	*Crya2*	H3143B04	Inhibitor of NF-κB	−3.921	3.479
Signal transduction					
Adenylate kinase†	*Ak2*	H3052D11		−3.755	3.546
Max dimerization protein 4†*	*Mad4*	H3131B07		−2.008	2.131
MAD homolog 4	*Madh4*	H3128C04		−2.765	2.114
*NF-κB enhancer inhibitor**	*Nfkbia*	H3026A08		−1.433	4.611
NIK-related kinase	*Nrk*	H3008B02	Activates NF-κB	−2.244	4.859
*Phosphoglycerate kinase**	*Pgk1*	H3023D06		−2.659	2.061
Protein tyrosine phosphatase4	*Ptp4a2*	H3088F03		−2.118	1.615
Rho-associated coiled-coil	*Rock1*	H3069C09		−2.808	3.183
TNF receptor associated factor	*Traf1*	H3015E06	NF-κB dependent	−2.011	1.243
Nuclear proteins/transcription factors					
Cbp/p300 interacting transactivation	*Cited4*	H3076H08	NF-κB co-activator	−2.178	2.745
High mobility group box 1	*Hmgb1*	H3126A05	Binds p50 subunit	−3.104	1.739
Jun oncogene	*Jun*	H3058C09	NF-κB co-activator	−2.906	2.057
Ras-related C3	*Rac1*	H3018C09	Inducer of NF-κB	−2.004	3.329
RNA processing					
Nuclear protein 220†	*Np220*	H3029A07		−2.259	1.827
*RNA polymerase II**	*Rpo2-3*	H3055H08	Co-activator of p65	−2.639	4.501
Protein synthesis/modification					
Eukaryotic translation 4g2	*Eif4g2*	H3113E10		−4.698	2.222
*Nedd4 WW-binding protein 4**	*N4wbp4*	H3062G06		−6.966	2.814
Structural proteins					
α 2 glycoprotein 1†*	*Azgp1*	IMAGE:521249		−2.013	1.398
β spectrin 2†*	*Spnb2*	H3010G09		−3.781	1.015
*Catenin β**	*Catnb*	H3031E05	Regulated by IKK	−3.998	3.061
Fibronectin†	*Fn1*	H3116A10		−6.201	4.723
Catenin α 1†*	*Catna1*	H3018E08		−1.996	1.723
Tenascin C	*Tnc*	L0062E01		−2.557	1.956
Other					
Deleted in polyposis	*Dp1*	J0420H06		−2.473	2.137
Insulin-like growth factor r2	*Igfr2*	H3148G08		−2.765	2.494
*Ninjurin 1**	*Ninj1*	H3072B10		−2.579	4.878
Rabaptin 5†*	*Rab5ep*	H3002C01		−2.739	1.333
Topoisomerase II α†*	*Top2a*	H3139A05	Inducer of NF-κB	−2.427	2.893
Tumor differentially expressed†	*Tde11*	H3014H10		−2.593	1.18
*WW domain binding 5**	*Wbp5*	H3127H02		−2.087	3.313
Zinc finger protein 68†*	*Zfp68*	H3058F07		−4.122	5.885

NOTE. Number of genes regulated by NF-κB = 47/141. Number of genes previously associated with NF-κB = 39/141.

* Genes containing κB site in promoter region.

† Genes containing ACTACAG motif in coding sequence.

Downloaded from http://aacrjournals.org/cancerres/article-pdf/64/18/6511/2518426/zch01804006511.pdf by guest on 01 March 2024

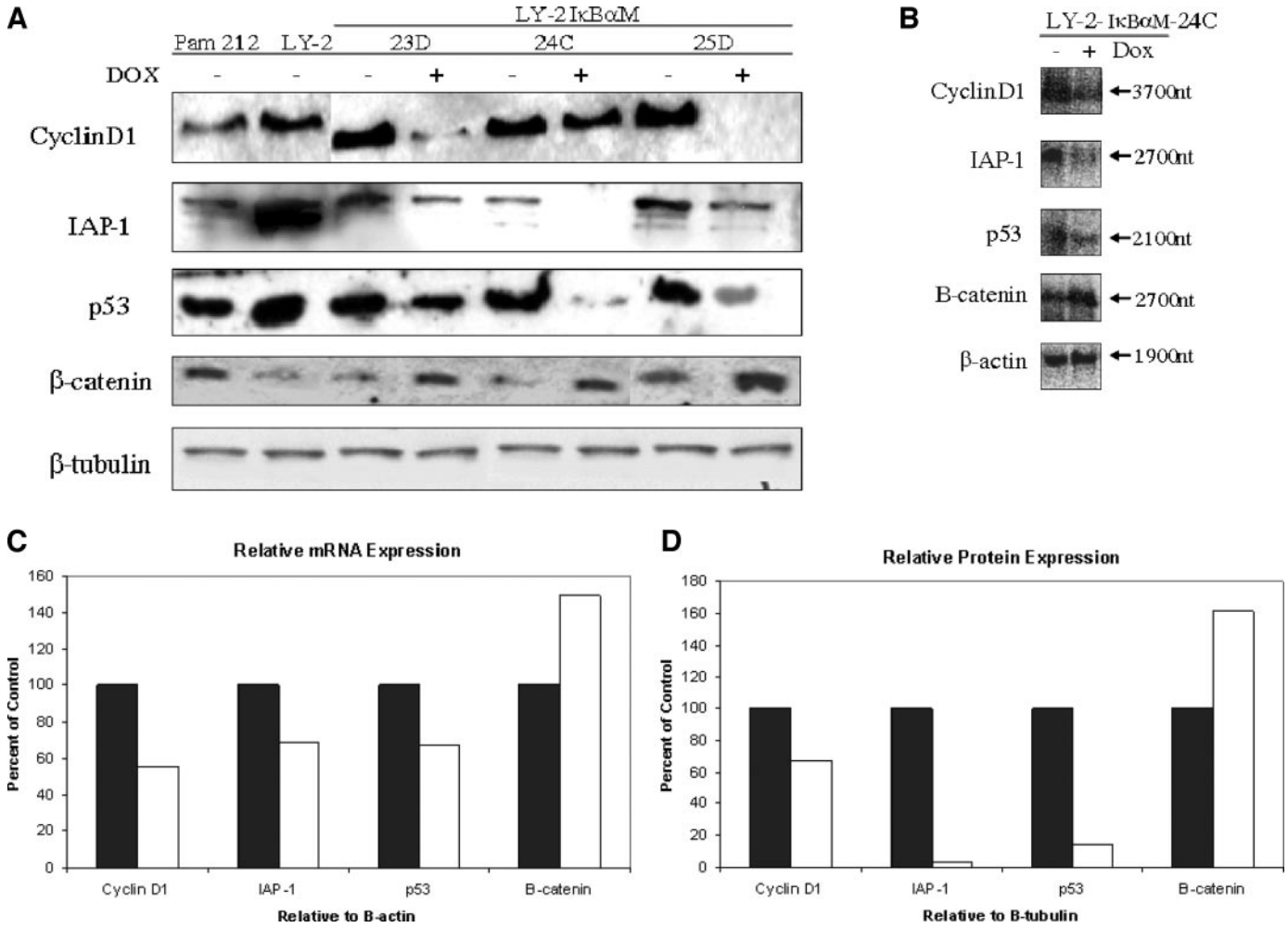

Fig. 3. Expression of cyclin D1, IAP-1, Trp53, and β-catenin with tumor progression and after suppression of NF-κB activation by IκBαM. *A*, Western blot analysis of protein expression in Pam 212 and LY-2 control and in LY-2 IκBαM clones 23D, 24C, and 25D ± DOX. Increased protein expression of cyclin D1, IAP-1, and Trp53 and decreased expression of β-catenin with increased activation of NF-κB were observed in LY-2 cells relative to Pam 212 cells. Cyclin D1, IAP-1, and Trp53 protein expression is inhibited and β-catenin expression is increased in LY-2 IκBαM clones after DOX-induced expression of IκBαM. β-Tubulin served as a control for loading and integrity of protein. *B*, Northern blot analysis of mRNA expression in LY-2 24C Tet IκBαM ± DOX. The mRNA expression of *cyclin D1*, *Trp53*, and *IAP-1* is inhibited in LY-2 24C cells after DOX-induced expression of IκBαM. Levels of *β-catenin* mRNA are increased in LY-2 24C cells after DOX-induced expression of IκBαM. *β-Actin* serves as a control for loading and integrity of mRNA. *C* and *D*, densitometric comparison of protein and mRNA expression of cyclin D1, IAP-1, Trp53, and β-catenin. The percentage difference in protein and mRNA expression between −DOX and +DOX normalized to constitutive controls is shown. ■, 24C−; □, 24C+.

(15–19), consistent with increased activation of NF-κB (5) in LY-2 SCC cells (Tables 1 and 2).

To validate the expression profile of *cyclin D1*, *Trp53*, *IAP-1*, and *β-catenin* detected in LY-2 cells and that obtained after modulation of NF-κB by IκBαM, expression was compared by Western and Northern blot analysis using protein and mRNA extracts from samples obtained after 72 hours of culture ± DOX, concurrent with array experiments shown in Fig. 1. Fig. 3*A* shows Western blots comparing cyclin D1, Trp53, IAP-1, and β-catenin protein expression in the low NF-κB Pam 212, high NF-κB LY-2 cells and in three LY-2 IκBαM clones ± DOX. Compared with Pam 212, LY-2 cells and most of the LY-2 IκBαM clones without DOX showed increased cyclin D1, IAP-1, and Trp53 and decreased β-catenin protein expression levels, consistent with the profiles obtained by array. Conversely, with inhibition of NF-κB by IκBαM in the LY-2 clones + DOX, decreased expression of cyclin D1, Trp53, and IAP-1 and increased expression of β-catenin proteins are observed in most clones, consistent with modulation of the genes encoding these proteins. There were no differences due to differences in loading or NF-κB activation between cell lines when blots were probed for the constitutively expressed protein β-tubulin. Thus, the Western blot data are consistent with the role of NF-κB in the modulation of these genes in LY-2 cells detected by microarray.

To establish whether *cyclin D1*, *Trp53*, *IAP-1*, and *β-catenin* mRNA expression was modulated with NF-κB in LY2 IκBαM-expressing cells, Northern blot analysis was performed to compare mRNA expression by the LY2 IκBαM clone 24C cultured ± DOX. The Northern blots in Fig. 3*B* show that expression of IκBαM in LY-2 24C cells + DOX resulted in decreased mRNA signal for *cyclin D1*, *Trp53*, and *IAP-1* compared with LY-2 24C cells without DOX. In contrast, *β-catenin* mRNA expression was increased after expression of IκBαM in LY-2 24C cells + DOX. No nonspecific induction or degradation of mRNA or differences in loading were detected when blots were probed with *β-actin*. The differences in protein and mRNA expression for the LY2 IκBαM clone 24C cultured ± DOX are quantified and compared by densitometry in Fig. 3*C* and *D*. The direction of change for the proteins and genes studied is consistent for all four genes. The difference in protein and mRNA expression was similar for cyclin D1 and β-catenin, whereas the percentage difference for protein exceeds that observed for mRNA at the 72-hour time interval for IAP-1 and p53. Together, the Western and Northern blot data validate the expression profile detected by array for these known

Downloaded from http://aacrjournals.org/cancerres/article-pdf/64/18/6511/2518426/zch01804006511.pdf by guest on 01 March 2024

cancer-related genes in LY-2 cells and confirm that modulation of NF-κB by IκBαM results in up- or down-modulation of several NF-κB–regulated genes.

Because expression of wild-type *Trp53* has been reported to have proapoptotic rather than antiapoptotic effects, we performed a sequence analysis of *Trp53* in LY-2. This established the presence of nonconserved mutations in exons 6, codon 81, CCG (Pro) to CTG (Leu), and exon 7, codon 121, ATA (Ile) to ATG (Met), in *Trp53* in LY-2 SCC cells (data not shown). Thus, NF-κB appears to contribute to the overexpression of Trp53 in LY-2 SCC cells.

Nuclear Factor-κB–Related Motifs in the Promoter and Messenger RNA Coding Region of Genes Up- and Down-Regulated by Nuclear Factor-κB in Squamous Cell Carcinoma. To examine whether these and the larger list of genes modulated by IκBαM as detected by microarray contain DNA sequence motifs that are putative targets for NF-κB regulation, we performed a search of the DNA that included 2 kb of the promoter region and the full-length sequence of each gene. As annotated in Tables 1 and 2, multiple genes were identified that contain sequences for NF-κB DNA binding motifs (∗) and/or the ACTACAG 7-nucleotide motifs (#), recently shown to mediate posttranscriptional down-regulation of the genes *Myo D* and *Sox9* by NF-κB (13). Fully 105 of 167 (63%) of the genes classified as increased with tumor progression contained putative NF-κB promoter DNA binding sequences, approximating the percentage of ~69% found to be down-modulated by IκBαM (see Table 1, Genes Increased with Tumor Progression). These include *cyclin D1*, *Trp53*, and *IAP-1* confirmed by Western and Northern blot analysis. Of the genes decreased with tumor progression (Table 2), 47 of 141 (33%) also contained NF-κB DNA binding motifs, including *β-catenin.* The DNA binding motif associated with p65 RelA (12) expressed in LY-2 and other SCCs was present in 42% of the genes showing increased expression but in only 14% of the genes showing decreased expression. Overall, NF-κB (63%) and p65 (42%) DNA binding motifs were increased in LY-2 cells with tumor progression when compared with NF-κB motifs detected in 25% of 900 genes randomly selected from the array list, indicating that the increase in representation of these motifs in genes expressed is unlikely to have occurred by chance (χ^2, $P < 0.001$).

The motif ACTACAG shown to be involved in posttranscriptional down-regulation of the genes *MyoD* and *Sox9* by NF-κB (13) was detected in the promoter, exon, or intronic DNA sequence of over 50% of genes exhibiting decreased expression with tumor progression, but these motifs were present at a similar frequency in the DNA of genes showing increased expression and in 10^4 genes selected randomly and analyzed by the National Center for Bioinformatics (χ^2, $P > 0.05$). The 7-mer motif was present in the coding portion of 30 of 167 (17%) and 18 of 141 (13%) genes showing increased or decreased expression, respectively. When only those genes that contain the 7-mer within the coding sequence and in-frame as found in *MyoD* and *Sox9* (13) are included, we detected this motif in 14 of 167 genes increased with tumor progression and 11 of 141 genes decreased with tumor progression, a frequency of ~8%.

Fig. 4 shows the alignment of the ACTACAG motif and adjacent DNA sequences for genes that showed conserved nucleotides with those of *MyoD* and *Sox9* and/or within the same region of their human homologues (∗). Cytosines (*C*) located 5 and/or 8 nucleotides 5′ and after the 7-mer and C or G nucleotides (*S*) located 10, 13, 14, and 16 nucleotides 3′ to the motif were most common. Although these homologies suggest a possible relationship to the mRNA regulatory motifs found in *MyoD* and *Sox9*, all but *Atp11a* lacked multiple repeats, and *Fn1* contained a motif not found in its human homologue. Thus, whereas the NF-κB DNA binding sequences involved in transcriptional regulation are significantly increased in genes differentially

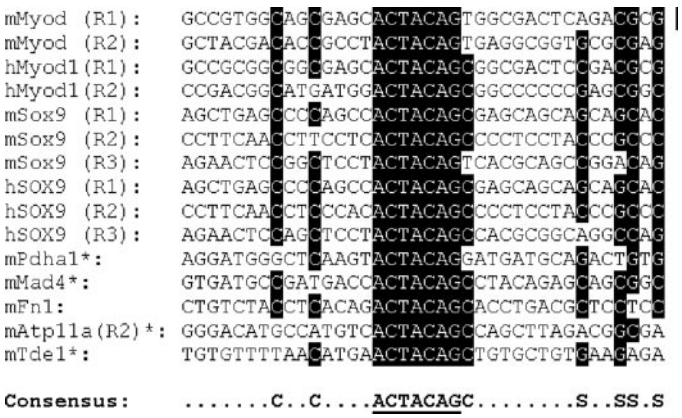

Fig. 4. Comparison of ACTACAG motifs and adjacent DNA sequences between MyoD, Sox9, and selected genes detected by array showing conserved nucleotides. The coding sequences of MyoD, Sox9, and a panel of selected genes were aligned with reference to the ACTACAG motif. Conserved nucleotides among the sequences are *shaded*. *S* represents C or G. *Asterisk* indicates that homologous nucleotides were present in the same region in corresponding human sequences.

expressed in SCC, the significance and functional role of ACTACAG motifs found in the genes detected remain to be determined.

Effect of Inhibition of Nuclear Factor-κB on the Malignant Phenotype of Squamous Cell Carcinoma. The putative functional role of the validated genes and other genes in Tables 1 and 2 in cell proliferation and death, inflammation/angiogenesis, migration/metastasis, metabolism, stress, signaling, gene and protein expression, and structure is consistent with the complex phenotypic differences between keratinocytes and highly metastatic SCC cells. To establish whether the modulation by NF-κB is associated with effects on the malignant phenotype, we examined the effect of modulation of IκBαM on several features of malignancy in LY-2 cells. DOX-induced expression of IκBαM had minor effects on proliferation beginning at day 3 as measured by MTT densitometric assay (Fig. 5*A*), corresponding to the interval when DOX-induced inhibition of NF-κB activation was detected (Fig. 1*A*). No changes in cell morphology, trypan blue uptake, or detachment were evident on microscopy (data not shown). To determine whether the decreased density observed by day 5 was related to cell death, cell cultures were examined by microscopy and by DNA cytofluorometry for cell cycle changes and subcellular DNA fragmentation that are produced on cell death. Cells expressing IκBαM began to show blebbing, fragmentation and detachment (data not shown). This was accompanied by the loss of DNA from G, S, and M phases and shift of ~50% of the DNA to the sub–G_0-G_1 fraction, consistent with cell death and fragmentation (Fig. 5*B*).

Because a number of genes potentially involved in cell adhesion, migration, and invasion were identified by array, we compared the migration and invasion of Pam 212 and LY-2 cells and examined the effect of inhibition of NF-κB on migration and invasion through Matrigel matrix in a two-chamber assay between 24 and 72 hours after addition of DOX, before significant cell loss or death was detected. Fig. 6*A* shows that control LY-2 cells ± DOX exhibit a similar increase in invasion of matrix relative to Pam 212. However, the invasiveness of four of four LY-2 clones conditionally expressing IκBαM was reduced to levels at or below those observed for Pam 212, suggesting that the increase in NF-κB observed in LY-2 cells plays a role in the increased migration and invasiveness of these metastatic cells.

Because NF-κB regulates Gro-1, a factor that promotes tumorigenesis and host angiogenesis (5, 14), the effect of inhibition of NF-κB by IκBαM on tumorigenesis and angiogenesis was examined. Fig. 6*B* shows the tumor growth of control LY-2 cells and the LY-2 clone 24C

Downloaded from http://aacrjournals.org/cancerres/article-pdf/64/18/6511/2518426/zch01804006511.pdf by guest on 01 March 2024

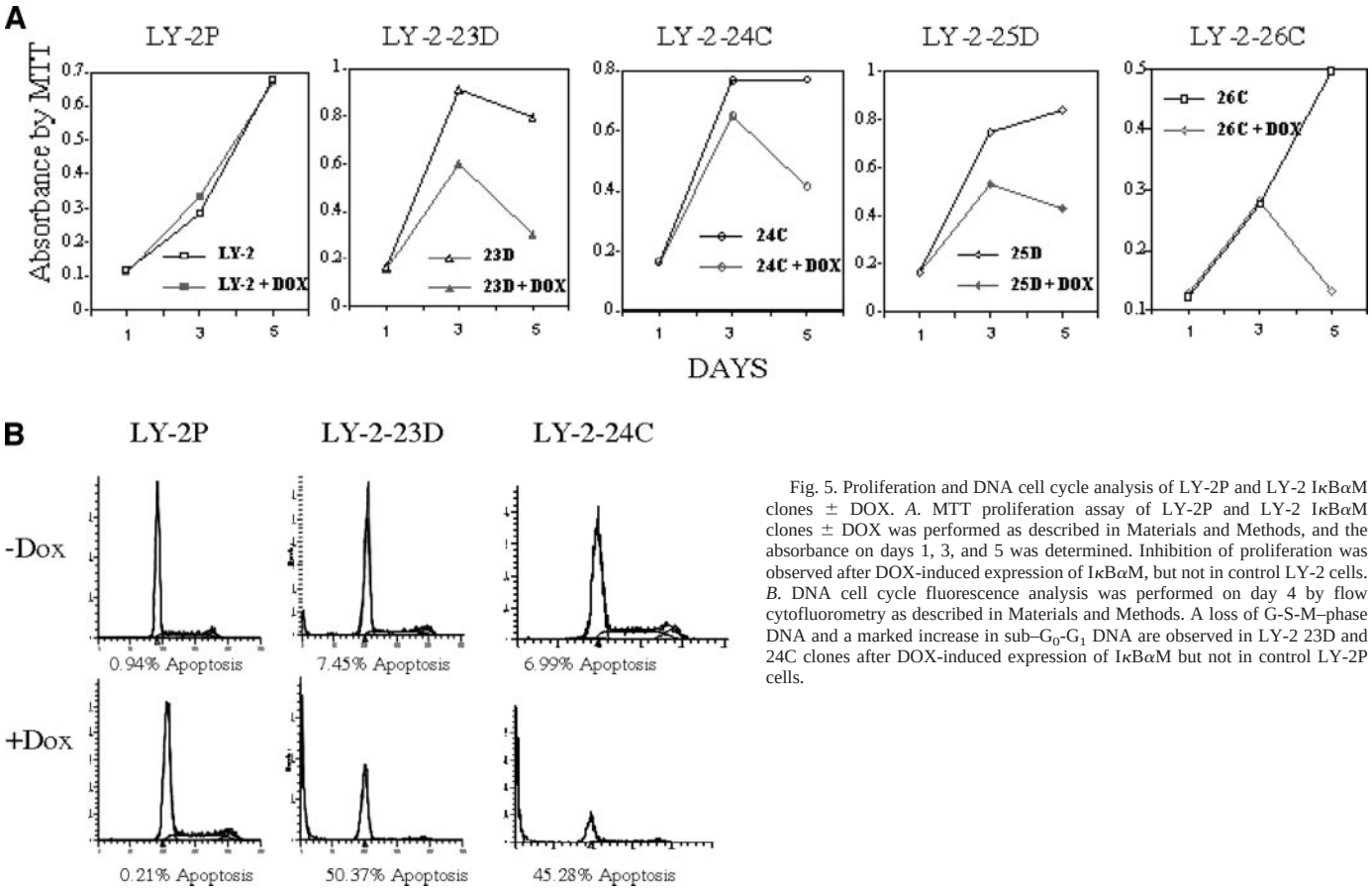

Fig. 5. Proliferation and DNA cell cycle analysis of LY-2P and LY-2 IκBαM clones ± DOX. *A.* MTT proliferation assay of LY-2P and LY-2 IκBαM clones ± DOX was performed as described in Materials and Methods, and the absorbance on days 1, 3, and 5 was determined. Inhibition of proliferation was observed after DOX-induced expression of IκBαM, but not in control LY-2 cells. *B.* DNA cell cycle fluorescence analysis was performed on day 4 by flow cytofluorometry as described in Materials and Methods. A loss of G-S-M–phase DNA and a marked increase in sub–G_0-G_1 DNA are observed in LY-2 23D and 24C clones after DOX-induced expression of IκBαM but not in control LY-2P cells.

before and after addition of DOX to the drinking water of congenic BALB/c SCID mice. On addition of DOX (*arrow*), the parental line continued to grow, whereas LY-2 24C tumor rapidly regressed with inhibition of NF-κB by IκBαM. No regrowth was detected in mice undergoing complete regression, but four mice retained small palpable nodules. To determine whether the inhibition was associated with decreased angiogenesis, the density of CD31-expressing blood vessels in the control and four mice bearing residual 24C tumors was compared. Fig. 6*C* illustrates the difference in tumor size in H&E-stained specimens and the associated difference in density of CD31 staining vessels. The microvessel density was significantly reduced in 24C tumors compared with control LY-2 tumors treated with DOX (53 ± 15 *versus* 175 ± 23, mean number of vessels per high-powered field ± SD; $n = 4$; $P < 0.05$). The clone transfected with IκBαM grew more slowly than the parental control, even in the absence of DOX. This slower tumor formation was associated with a ~10% to 30% lower expression of NF-κB-modulated angiogenesis factors Gro-1 and vascular endothelial growth factor in 24C and other clones compared with parental LY-2 cells, suggesting a degree of "leakiness" and weak suppression of NF-κB-inducible genes by the Tet-inducible promoter, even in the absence of DOX (data not shown).

DISCUSSION

In this study, we obtained evidence for differential expression of a diversity of known NF-κB–related genes and provide evidence that modulation of the NF-κB pathway directly or indirectly modulates a significant portion of these and other genes in the molecular profile altered with malignant progression in a syngeneic model of SCC. The array profile obtained with the expanded 15,000-element microarray reproduced differences in expression of a number of NF-κB–related genes detected and validated by Northern blot in our previous study, as well as other genes reported to be differentially expressed and important in oncogenesis of SCC. We confirmed that IκBαM expression suppressed NF-κB reporter and DNA binding activity and modulated protein and mRNA expression of several putative NF-κB target genes differentially expressed in SCC, including *cyclin D1*, *Trp53*, *IAP-1*, and *β-catenin* (15–19). Bioinformatic analysis revealed that the sequence of these and many of the other putative NF-κB–modulated genes contain promoter or coding sequences homologous to the NF-κB DNA binding motif or an ACTACAG 7-nucleotide motif recently shown to mediate posttranscriptional down-regulation by NF-κB of *MyoD* and *Sox9* mRNA expression (13). Consistent with the diversity and putative function of many of these genes, inhibition of NF-κB was found to inhibit proliferation, cell survival, migration, angiogenesis, and tumorigenesis. These results provide evidence that NF-κB is an important modulator of the gene expression profile and malignant phenotype in SCC and provide an expanded list of candidate genes potentially modulated directly or indirectly by NF-κB to be investigated in future studies.

Homologues of several of the genes detected with malignant progression and modulated by NF-κB in this murine SCC model have been found to be differentially expressed and important in oncogenesis in human SCCs. *Cyclin D1* is overexpressed in the majority of human head and neck squamous cell carcinoma (HNSCCs) and promotes proliferation and tumorigenesis (20). *Cyclin D1* overexpression results from gene amplification in only a minority of SCCs, and the results of this study provide evidence that NF-κB activation can contribute to the overexpression of *cyclin D1* in SCCs. The tumor

Downloaded from http://aacrjournals.org/cancerres/article-pdf/64/18/6511/2518426/zch01804006511.pdf by guest on 01 March 2024

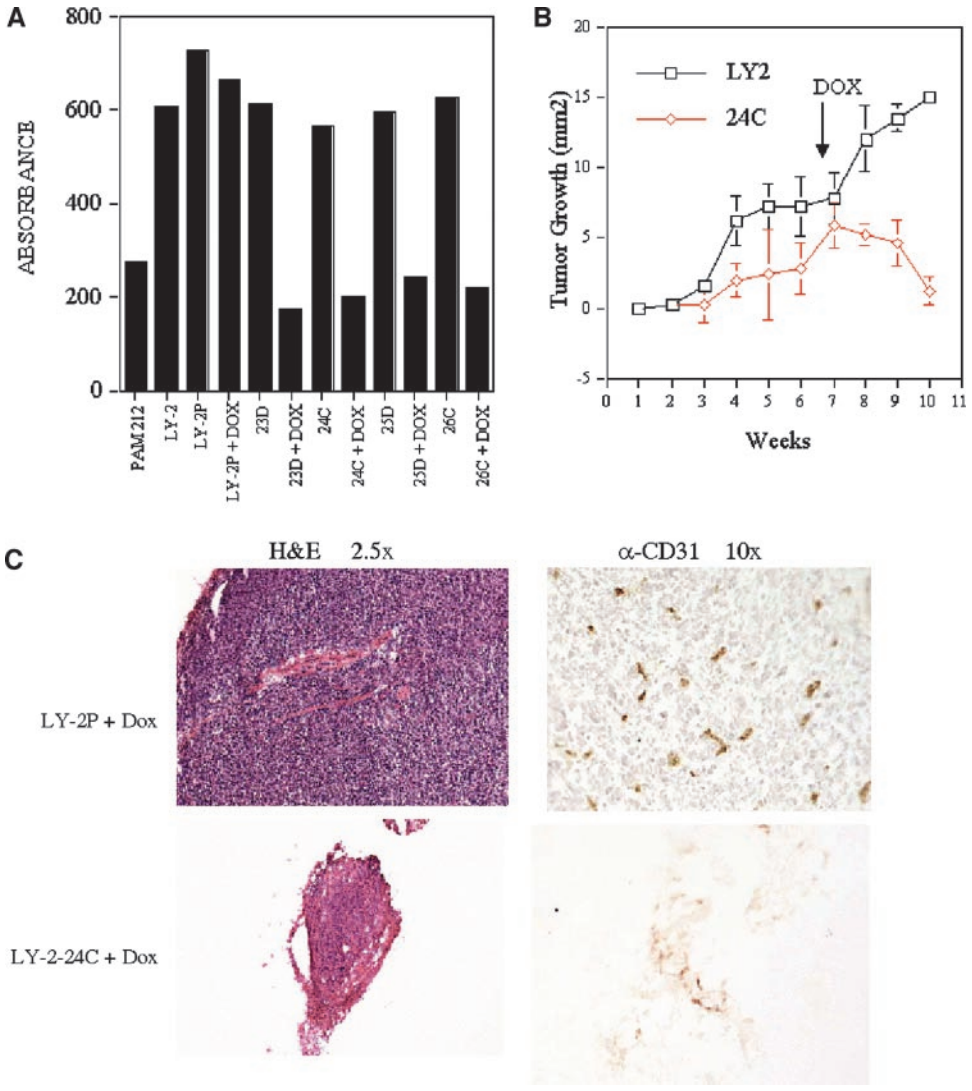

Fig. 6. Effect of inhibition of NF-κB by IκBαM on invasion, tumorigenesis, and angiogenesis. *A*, two-chamber invasion assay. Relative invasiveness as measured by absorbance of cells invading through matrix to the lower chamber is correlated with the relative differences in metastatic potential and NF-κB activation of transformed Pam 212, metastatic Pam LY-2, and LY-2P cells. The increased invasiveness of LY-2 IκBαM clones in the absence of DOX is reduced after induction of IκBαM. *B*. Tumor growth of LY-2 and LY-2 24C in BALB/c SCID mice before and after addition of DOX to drinking water. LY-2 24C grows more slowly than LY-2 and regresses after induction of IκBαM by DOX. *C*, comparison of histology and microvessel density of LY-2P and LY-2 24C tumors at week 10. H&E staining shows decreased cellular density and size of LY-2 24C tumors relative to LY-2P tumors. CD31 staining shows decreased microvessel density of LY-2 24C tumors relative to LY-2P tumors.

suppressor *Trp53* is mutated and overexpressed in approximately half of human HNSCCs and plays an important role in cell cycle arrest and DNA repair or apoptosis (21). The overexpression of *Trp53* in LY-2 and inhibition after inactivation of NF-κB suggest that NF-κB may contribute to overexpression of *Trp53*. Increased expression of *IAP-1* (Birc2) was previously detected in metastatic SCC (4). The inhibition of *IAP-1* expression with inhibition of NF-κB in this study is consistent with the effect of inhibition of NF-κB in sensitizing LY-2 cells to apoptosis and HNSCC to tumor necrosis factor-induced caspase-mediated cell death (22). Decreased expression of *β-catenin* has been observed and associated with metastasis of human oral SCC (23). The low expression of *β-catenin* in metastatic LY-2 cells relative to keratinocytes and restoration of increased mRNA and protein levels after expression of IκBαM suggest that repression of *β-catenin* expression can result from NF-κB activation in SCC. The effects of modulation of NF-κB on expression of *cyclin D1*, *Trp53*, *IAP-1*, and *β-catenin* observed in this study are consistent with those observed with modulation of NF-κB in other malignancies (15–19).

When the expression of the four genes was compared by microarray and Northern and Western blots, the direction of change for the proteins and genes studied was consistent for all four genes (Fig. 3*C* and *D*). The percentage change was similar for protein and mRNA for cyclin D1 and β-catenin, whereas the percentage difference for protein was greater than that observed for mRNA at the 72-hour time interval for IAP-1 and p53. These differences between protein and mRNA could be due to a variety of mechanisms for individual genes. These include differences in kinetics related to other IκBs (24), kinetics of modulation of RNA and protein, differences in stability and posttranscriptional processing of RNA, or differences in efficiency of translation. It will be important to determine whether differences among genes are due to different regulatory mechanisms in future studies.

Bioinformatic analyses of the four validated genes for NF-κB–related motifs reveal that the sequences of the *cyclin D1*, *Trp53*, *IAP-1*, and *β-catenin* promoters contain NF-κB DNA binding motifs. The sequence of *β-catenin* also contains an ACTACAG 7-nucleotide motif in the noncoding portion of the gene. The presence of this motif in the coding region has recently been shown to mediate posttranscriptional down-regulation by NF-κB of *MyoD* and *Sox9* mRNA expression (13), but the role of the motif located in the noncoding portion of β-catenin remains to be determined. Although we have obtained evidence that NF-κB modulates these and a wider profile of genes containing these motifs in Tables 1 and 2, it will be necessary to determine individually for each gene by mutagenesis whether gene expression is regulated directly by NF-κB or indirectly by other transcription factors or regulatory molecules also modulated during the 72-hour interval required for significant DOX-induced expression of IκBαM and inhibition of NF-κB.

Downloaded from http://aacrjournals.org/cancerres/article-pdf/64/18/6511/2518426/zch01804006511.pdf by guest on 01 March 2024

Gro-1, one of the genes consistently detected in LY-2 and aggressive SCC in this and previous studies, was also previously shown to be modulated by NF-κB and to contribute to angiogenesis, tumorigenesis, and metastasis (5, 14). We showed that enforced expression of *Gro-1* in low-*Gro-1*–expressing Pam 212 cells converted these cells to the LY phenotype and promoted increased angiogenesis, tumorigenesis, and metastasis, indicating that this NF-κB–regulated gene contributes directly to the malignant phenotype of SCC in this model (14). Conversely, we show in this study that inhibition of NF-κB and *Gro-1* expression in LY-2 cells overexpressing *Gro-1* is associated with decreased angiogenesis and tumorigenesis. Human cytokine GRO1 and its homologue, interleukin-8, have been found to be overexpressed in the majority of HNSCCs and many other cancers (3, 25). Consistent with the effects of inhibition of NF-κB by IκBα on gene expression and phenotype observed in this study, constitutive expression of an IκBα mutant in human HNSCC inhibited expression of interleukin-8 and tumorigenesis of xenografts in mice (7). Although the results suggest an important functional role of NF-κB in angiogenesis and tumorigenesis, the decrease in angiogenesis observed could be due in part to apoptosis and reduction in tumor mass producing angiogenesis factors, as well as decreased transcription.

Our previous studies and the present molecular profiling study of malignant progression reveal differences in expression of a variety of other putative NF-κB–modulated genes that are consistent with expression patterns observed more broadly in SCC. Glutathione *S*-transferase was increased in LY-2 and inhibited with suppression of NF-κB activation. Overexpression of glutathione *S*-transferases involved in metal metabolism has been detected and shown to be important in resistance of SCC to *cis*-platinum and other chemotherapy agents (26). Expression of the cell adhesion molecules integrin $\alpha_3\beta_1$ and decreased expression of cadherin 1 and β-catenin protein are often observed and associated with poor prognosis in SCC and other epithelial cancers (2, 23). Decreased expression of the cell-cell receptor Ly-6 was also confirmed previously in LY SCC cells (27). Finally, the detection of several classes of molecules previously detected as tumor specific and tumor-associated antigens in SCC such as Ly-6, integrins, DEAD-box helicases, and ribosomal components (2, 27–29) suggests that NF-κB may contribute to expression of antigenic molecules detected by antibodies and T cells. Identification of NF-κB–regulated genes could help determine the identity of antigens for immune therapy as well as their function in the malignant phenotype. The differences in expression of these candidates implicated in regulation of resistance to chemotherapy-induced apoptosis, adhesion, and immune antigenicity in this model are therefore consistent with broader expression in SCC and make the role of NF-κB in their regulation of broader potential relevance.

We noted in the previous study with a first-generation 4,000-element murine array that a significant portion of the genes overexpressed in multiple metastatic reisolates were reported to be related to the NF-κB pathway. Consistent with this, a search of PubMed revealed that >40% of the up-regulated genes and ~28% of the down-regulated genes detected in LY-2 with the 15,000-element array in the present study were related previously to NF-κB. The detection of both known and additional up- and down-regulated genes with modulation of NF-κB prompted us to undertake an analysis to determine whether the genes identified contained common regulatory motifs related to NF-κB. Bioinformatic analysis of the sequence of genes detected with tumor progression of LY-2 in this study revealed that 63% of the genes increased in LY-2 cells contained NF-κB binding motifs in the promoter region. Of the candidates showing lower expression, 33% contained NF-κB binding motifs, and ~8% contained one or more motifs found in *MyoD* and *Sox9* mRNA implicated in NF-κB–mediated posttranscriptional down-regulation (13). The detection of sequences homologous to the 7-nucleotide motif detected in *MyoD* and *Sox9* mRNA suggests that this NF-κB–regulated mechanism may be involved in down-regulation of other genes besides *MyoD*. The restoration of expression of these genes back up to the levels observed in keratinocytes after expression of IκBαM in LY-2 provides support for this hypothesis. The mechanism underlying NF-κB modulation of *MyoD* and *Sox9* mRNA and relevance to expression of other genes in cancer remain to be established.

Cumulative evidence in head and neck, lymphoid, breast, gastric, colorectal, and prostate cancers is consistent with the hypothesis that NF-κB is constitutively activated and a major "culprit" in the pathogenesis of cellular and host alterations in these cancers (reviewed in refs. 25 and 30). NF-κB has been implicated in the oncogenesis of a number of other malignancies, indicating that NF-κB activation may be a common pathway of broad importance in cancer (30). Viral and cellular members of the NF-κB family have been shown to be transforming (31, 32), and oncogenic activation of RAS, ABL, LMP-1, interleukin-1, and epidermal growth factor receptor has been shown to contribute to activation of NF-κB in different cancers (10, 33–36). Constitutive activation of NF-κB and NF-κB–inducible genes has been detected in prostate and breast cancers, melanomas, and lymphomas (25, 37–41). NF-κB has been implicated in promoting expression of the phenotypic changes and genes involved in inhibition of programmed and therapeutic cell death (18, 22, 41–44), proliferation (15), tumorigenesis (7, 25, 34), angiogenesis, invasiveness, and metastatic potential (9, 25, 38).

Furthermore, molecular profiling has revealed that NF-κB may regulate a diverse repertoire of genes in SCC (this study) and in Hodgkin's and non-Hodgkin's lymphomas (39–41). We have provided evidence that NF-κB modulates many of the genes and phenotypic features differentially regulated during malignant progression in this stepwise model of SCC. The broader significance of these results is independently supported by our earlier results showing that NF-κB is activated in multiple murine and human SCCs (2, 5, 6) and that constitutive inhibition of NF-κB in human SCC inhibits cell survival, angiogenesis factor expression, and growth of xenografts (7, 9). The genes detected represent programs that are functionally involved in many of the phenotypic features that constitute the hallmarks of cancer (1). These results suggest that NF-κB is a key molecular switch of the alterations in genotype and phenotype in malignant progression of SCC. Increasing appreciation of the role of NF-κB in regulation of expression of a diversity of genes in cancer is consistent with the evolutionarily importance of this transcription factor in regulating programmed or stereotyped gene responses to injury and pathogens (25, 30).

REFERENCES

1. Hanahan D, Weinberg RA. The hallmarks of cancer. Cell 2000;100:57–70.
2. Van Waes C, Surh DM, Chen Z, et al. Increase in suprabasilar integrin adhesion molecule expression in human epidermal neoplasms accompanies increased proliferation occurring with immortalization and tumor progression. Cancer Res 1995;55:5434–44.
3. Chen Z, Malhotra PS, Thomas GR, et al. Expression of proinflammatory and proangiogenic cytokines in patients with head and neck cancer. Clin Cancer Res 1999;5:1369–79.
4. Dong G, Loukinova E, Chen Z, et al. Molecular profiling of transformed and metastatic murine squamous carcinoma cells by differential display and cDNA microarray reveals altered expression of multiple genes related to growth, apoptosis, angiogenesis, and the NF-kappaB signal pathway. Cancer Res 2001;61:4797–808.
5. Dong G, Chen Z, Kato T, Van Waes C. The host environment promotes the constitutive activation of nuclear factor-kappaB and proinflammatory cytokine expression during metastatic tumor progression of murine squamous cell carcinoma. Cancer Res 1999;59:3495–504.
6. Ondrey FG, Dong G, Sunwoo J, et al. Constitutive activation of transcription factors NF-kappaB, AP-1, and NF-IL6 in human head and neck squamous cell carcinoma cell lines that express pro-inflammatory and pro-angiogenic cytokines. Mol Carcinog 1999;26:119–29.

Downloaded from http://aacrjournals.org/cancerres/article-pdf/64/18/6511/2518426/zch01804006511.pdf by guest on 01 March 2024

7. Duffey DC, Chen Z, Dong G, et al. Expression of a dominant-negative mutant inhibitor-kappaBalpha of nuclear factor-kappaB in human head and neck squamous cell carcinoma inhibits survival, proinflammatory cytokine expression, and tumor growth in vivo. Cancer Res 1999;59:3468–74.
8. Karin M, Delhase M. The IkappaB kinase (IKK) and NF-kappa B: key elements of proinflammatory signaling. Semin Immunol 2000;12:85–98.
9. Sunwoo JB, Chen Z, Dong G, et al. Novel proteasome inhibitor PS-341 inhibits activation of nuclear factor-kappaB, cell survival, tumor growth, and angiogenesis in squamous cell carcinoma. Clin Cancer Res 2001;7:1419–28.
10. Bancroft CC, Chen Z, Yeh J, et al. Effects of pharmacologic antagonists of epidermal growth factor receptor, PI3K and MEK signal kinases on NF-kappaB and AP-1 activation and IL-8 and VEGF expression in human head and neck squamous cell carcinoma lines. Int J Cancer 2002;99:538–48.
11. Chen Z, Smith CW, Kiel D, Van Waes C. Metastatic variants derived following in vivo tumor progression of an in vitro transformed squamous cell carcinoma line acquire a differential growth advantage requiring tumor-host interaction. Clin Exp Metastasis 1997;15:527–37.
12. Kunsch C, Ruben SM, Rosen CA. Selection of optimal kappaB/Rel DNA binding motifs: interaction of both subunits of NF-kappaB with DNA is required for transcriptional activation. Mol Cell Biol 1992;12:4412–21.
13. Sitcheran R, Cogswell PC, Baldwin AS Jr. NF-kappaB mediates inhibition of mesenchymal cell differentiation through a posttranscriptional gene silencing mechanism. Genes Dev 2003;17:2368–73.
14. Loukinova E, Dong G, Enamorado-Ayalya I, et al. Growth regulated oncogene-alpha expression by murine squamous cell carcinoma promotes tumor growth, metastasis, leukocyte infiltration and angiogenesis by a host CXC receptor-2 dependent mechanism. Oncogene 2000;19:3477–86.
15. Hinz M, Krappmann D, Eichten A, et al. NF-kappaB function in growth control: regulation of Cyclin D1 expression and G_0/G_1-to-S-phase transition. Mol Cell Biol 1999;19:2690–8.
16. Guttridge DC, Albanese C, Reuther JY, Pestell RG, Baldwin AS Jr. NF-kappaB controls cell growth and differentiation through transcriptional regulation of Cyclin D1. Mol Cell Biol 1999;19:5785–99.
17. Chen W, Cooper NR. Epstein-Barr virus nuclear antigen 2 and latent membrane protein independently transactivate Trp53 through induction of NF-kappaB activity. J Virol 1996;70:4849–53.
18. Wang CY, Mayo MW, Korneluk RG, Goeddel DV, Baldwin AS Jr. NF-kappaB antiapoptosis: induction of TRAF1 and TRAF2 and c-IAP1 and c-IAP2 to suppress caspase-8 activation. Science (Wash DC) 1998;281:1680–3.
19. Masui O, Ueda Y, Tsumura A, et al. RelA suppresses the Wnt/beta-catenin pathway without exerting transcriptional ability. Int J Mol Med 2002;9:489–93.
20. Robles AI, Rodriguez-Puebla ML, Glick AB, et al. Reduced skin tumor development in cyclin D1-deficient mice highlights the oncogenic ras pathway in vivo. Genes Dev 1999;12:2469–74.
21. Taylor D, Koch WM, Zahurak M, et al. Immunohistochemical detection of Trp53 protein accumulation in head and neck cancer: correlation with Trp53 gene alterations. Hum Pathol 1999;30:1221–5.
22. Duffey DC, Crowl-Bancroft CV, Chen Z, et al. Inhibition of transcription factor nuclear factor-kappaB by a mutant inhibitor-kappaBalpha attenuates resistance of human head and neck squamous cell carcinoma to TNF-alpha caspase-mediated cell death. Br J Cancer 2000;83:1367–74.
23. Tanaka N, Odamjima T, Ogi K, Ikeda T, Satoh M. Expression of E-cadherin, alpha-catenin and beta-catenin in the process of lymph node metastasis in oral squamous cell carcinoma. Br J Cancer 2003;89:557–63.
24. Hoffmann A, Levchenko A, Scott ML, Baltimore D. The IkappaB-NF-kappaB signaling module: temporal control and selective gene activation. Science (Wash DC) 2002;298:1241–5.
25. Richmond A. Nf-kappaB, chemokine gene transcription and tumour growth. Nat Rev Immunol 2002;2:664–74.
26. Nishimura T, Newkirk K, Sessions RB, et al. Immunohistochemical staining for glutathione S-transferase predicts response to platinum-based chemotherapy in head and neck cancer. Clin Cancer Res 1996;2:1859–65.
27. Kato T, Dong G, Loukinova E, Chen Z, Van Waes C. Differential expression of the murine Ly-6A/E antigen homolog of human squamous cell carcinoma antigen E48 during malignant transformation and tumor progression of squamous cell carcinoma line Pam 212. Otolaryngol Head Neck Surg 1998;119:408–11.
28. Dubey P, Hendrickson RC, Meredith SC, et al. The immunodominant antigen of an ultraviolet-induced regressor tumor is generated by a somatic point mutation in the DEAD box helicase p68. J Exp Med 1997;185:695–705.
29. Beck-Engeser GB, Monach PA, Mumberg D, et al. Point mutation in essential genes with loss or mutation of the second allele: relevance to the retention of tumor-specific antigens. J Exp Med 2001;194:285–300.
30. Karin M, Cao Y, Greten FR, Li ZW. NF-kappaB in cancer: from innocent bystander to major culprit. Nat Rev Cancer 2002;2:301–10.
31. Gilmore TD. Multiple mutations contribute to the oncogenicity of the retroviral oncoprotein v-Rel. Oncogene 1999;18:6925–37.
32. Gilmore TD, Cormier C, Jean-Jacques J, Gapuzan ME. Malignant transformation of primary chicken spleen cells by human transcription factor c-Rel. Oncogene 2001; 20:7098–103.
33. Mayo MW, Wang CY, Cogswell PC, et al. Requirement of NF-kappaB activation to suppress Trp53-independent apoptosis induced by oncogenic Ras. Science (Wash DC) 1997;278:1812–5.
34. Reuther JY, Reuther GW, Cortez D, Pendergast AM, Baldwin AS Jr. A requirement for NF-kappaB activation in Bcr-Abl-mediated transformation. Genes Dev 1998;12: 968–81.
35. Laherty CD, Hu HM, Opipari AW, Wang F, Dixit VM. The Epstein-Barr virus LMP1 gene product induces A20 zinc finger protein expression by activating nuclear factor kappa B. J Biol Chem 1992;267:24157–60.
36. Wolf JS, Chen Z, Dong G, et al. Interleukin (IL)-1alpha promotes nuclear factor-kappaB and AP-1-induced IL-8 expression, cell survival, and proliferation in head and neck squamous cell carcinomas. Clin Cancer Res 2001;7:1812–20.
37. Sovak MA, Bellas RE, Kim DW, et al. Aberrant nuclear factor-kappaB/Rel expression and the pathogenesis of breast cancer. J Clin Investig 1997;100:2952–60.
38. Huang S, Pettaway CA, Uehara H, Bucana CD, Fidler IJ. Blockade of NF-kappaB activity in human prostate cancer cells is associated with suppression of angiogenesis, invasion, and metastasis. Oncogene 2001;20:4188–97.
39. Hinz M, Loser P, Mathas S, et al. Constitutive NF-kappaB maintains high expression of a characteristic gene network, including CD40, CD86, and a set of antiapoptotic genes in Hodgkin/Reed-Sternberg cells. Blood 2001;97:2798–807.
40. Hinz M, Lemke P, Anagnostopoulos I, et al. Nuclear factor kappaB-dependent gene expression profiling of Hodgkin's disease tumor cells, pathogenetic significance, and link to constitutive signal transducer and activator of transcription 5a activity. J Exp Med 2002;196:605–17.
41. Davis RE, Brown KD, Siebenlist U, Staudt LM. Constitutive nuclear factor kappaB activity is required for survival of activated B cell-like diffuse large B cell lymphoma cells. J Exp Med 2001;194:1861–74.
42. Wang CY, Mayo MW, Baldwin AS Jr. TNF- and cancer therapy-induced apoptosis: potentiation by inhibition of NF-kappaB. Science (Wash DC) 1996;274:784–7.
43. Beg AA, Baltimore D. An essential role for NF-kappaB in preventing TNF-alpha-induced cell death. Science (Wash DC) 1996;274:782–4.
44. Tergaonkar V, Pando M, Vafa O, Wahl G, Verma I. Trp53 stabilization is decreased upon NF-κB activation: a role for NFκB in acquisition of resistance to chemotherapy. Cancer Cell 2002;1:493–503.

Downloaded from http://aacrjournals.org/cancerres/article-pdf/64/18/6511/2518426/zch01804006511.pdf by guest on 01 March 2024